



# THE EFFECT OF ENTROPY NOISE ON COMBUSTION INSTABILITY IN THE PRESENCE OF ADVECTIVE SHEAR DISPERSION

Aimee S. Morgans and Jingxuan Li

*Department of Aeronautics, Imperial College London, UK*

*email: a.morgans@imperial.ac.uk*

When a flame burns unsteadily, two types of flow perturbation are generated. The first are acoustic waves, which propagate away from the flame at the speed of sound (relative to the flow), and are known as “direct combustion noise”. The second are temperature fluctuations, also known as hot/cold spots or entropy waves, which advect away from the flame with the local flow velocity. They are initially silent, but upon being accelerated generate new acoustic waves, known as “indirect combustion noise” or “entropy noise”. This can affect both combustion instability, via the upstream propagating component, and exhaust noise, via the downstream propagating component. The entropy noise generated depends crucially on the advection process between the flame, where the entropy wave is generated, and the combustor exit, where it is accelerated. New models for entropy wave advection have recently been developed, based on simplified turbulent channel flow simulations. These show that entropy waves do not dissipate, suffering only shear dispersion due to spatial variations in the time-averaged flow velocity; turbulent fluctuations have negligible effect. The effect of entropy noise on combustion instability in the context of this new advection model has not previously been considered, and is the topic of the present paper. The effect on combustor modes for mean turbulent velocity profiles exhibiting difference degrees of shear dispersion has been investigated. It is found that for a large range of practical combustors, spanning a representative range of combustor lengths, entropy noise in the presence of advective shear dispersion has the potential to strongly affect thermoacoustic modes.

---

## 1. Introduction

The introduction of lean premixed combustors in gas turbines has significantly reduced NO<sub>x</sub> emissions. However, this has rendered combustors more susceptible to thermoacoustic instabilities. Such instabilities arise due to the two-way coupling between the rate of combustion and the acoustic waves within the combustor. They lead to large amplitude self-excited oscillations, which have the potential to cause severe structural damage of the combustion chamber and its attached components.

Despite significant research interest, modelling and suppressing thermoacoustic instability remains an ongoing challenge. In terms of capturing one of the two mechanisms key to thermoacoustic instabilities – how the unsteady heat release rate of the flame generates acoustic waves – it is now widely recognised that there are two main mechanisms by which this can occur. The first is that unsteady heat release rate generates acoustic waves directly - these are often termed “direct combustion

noise”. The second concerns the temperature fluctuations, often called entropy waves, which are also generated by unsteady burning. These advect downstream – in a non-accelerating flow they have no noise associated with them. However, when they are accelerated, as happens upon leaving the combustor and entering the turbine in a gas turbine flow, acoustic waves are generated by the acceleration. These propagate both upstream and downstream [1] and are often termed “indirect combustion noise” or “entropy noise”. (Note that “indirect combustion noise” strictly includes both “entropy noise” and “vorticity noise” - the contribution from the former is assumed to dominate.)

The upstream-propagating component of entropy noise travels back into the combustor, where it causes further flame perturbations. It has recently been shown that it can have a significant effect on thermoacoustic instability, via effects such as mode destabilization, mode stabilization and mode switching [2]. The degree to which entropy noise affects the combustor thermoacoustic depends crucially on the entropy wave advection process that occurs prior to acceleration. That is, the advection of entropy waves between the flame, where they are generated, and the combustor exit/turbine inlet, where they are accelerated, dictates the degree to which entropy noise influences thermoacoustic instabilities. The above work [2] assumed a simplified dissipation-spread model for the entropy wave advection [3]. A new model for entropy wave advection has recently been developed, based on simplified turbulent channel flow simulations [4]. This suggests that entropy waves do not dissipate, suffering only shear dispersion due to spatial variations in the time-averaged flow velocity; turbulent fluctuations have negligible effect. The impulse response of the entropy wave strength between the flame and combustor exit is well modelled by a Gaussian-shaped profile, which can be deduced from the mean turbulent velocity profile, and also yields a Gaussian-shaped frequency response. The effect of entropy noise on combustion instability in the context of this new advection model has not previously been considered, and is the topic considered in the present paper.

In this work, we use a low order thermoacoustic network modelling tool, described in the next section, to systematically investigate the effect of entropy wave shear dispersion on thermoacoustic stability. Results for different combustor configurations are obtained and discussed.

## 2. Modelling Methodology

### 2.1 Low order network modelling

The thermoacoustic network modelling tool used is OSCIOS (v1.4), an open source tool, written in Matlab, and developed in the authors’ group [5, 6]. It is based on low-order network modelling for acoustic waves. The thermoacoustic system is represented as a network of simple (constant area) connected acoustic modules, as shown in Figure 1.

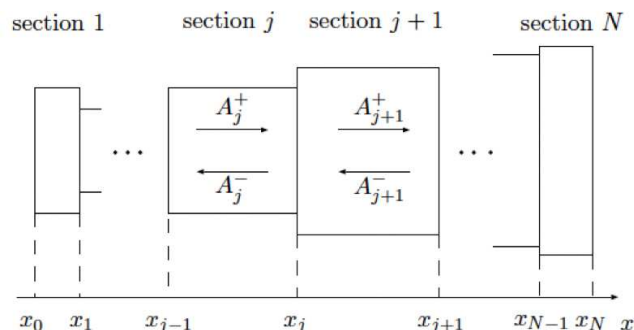


**Figure 1.** The low order modelling tool assumes a network of connected acoustic modules

Mean flow conditions change only across module interfaces - within each module they are constant. The acoustic wave behaviour is modelled analytically using linear wave-based methods. So,

for example, the pressure, density and velocity perturbations in a given module can be expressed in terms of upstream and downstream propagating acoustic wave strengths ( $A_j^+$  and  $A_j^-$ ) and an entropy wave strength ( $\sigma$ ).

$$(1) \quad p_j(x, t) = \bar{p}_j + A_j^+ \left( t - \frac{x}{\bar{c}_j + \bar{u}_j} \right) + A_j^- \left( t + \frac{x}{\bar{c}_j - \bar{u}_j} \right)$$

$$(2) \quad \rho_j(x, t) = \bar{\rho}_j + \frac{1}{\bar{c}_j^2} \left( A_j^+ \left( t - \frac{x}{\bar{c}_j + \bar{u}_j} \right) + A_j^- \left( t + \frac{x}{\bar{c}_j - \bar{u}_j} \right) \right) - \frac{\bar{\rho}_j}{c_p} \sigma \left( t - \frac{x}{\bar{u}_j} \right)$$

$$(3) \quad u_j(x, t) = \bar{u}_j + \frac{1}{\bar{\rho} \bar{c}} \left( A_j^+ \left( t - \frac{x}{\bar{c}_j + \bar{u}_j} \right) - A_j^- \left( t + \frac{x}{\bar{c}_j - \bar{u}_j} \right) \right)$$

Flow conservation equations are applied across module interfaces and acoustic boundary conditions are applied at the upstream and downstream ends of the system. The flame module is assumed to be acoustically compact (i.e. infinitely thin), so that the acoustic waves exhibit discontinuity in strength across the flame. Flow conservation equations are applied across the flame, and closure is provided by a flame model, which prescribes how the unsteady heat release rate of the flame responds to acoustic waves – this may be linear or non-linear. OSCILOS can provide predictions of the frequencies of resonant modes, their stability (positive or negative growth rate), mode shapes and the time evolution of disturbances. Non-linearity is assumed to arise only in the flame model. If a non-linear flame model has been used, non-linear effects such as limit cycle saturation amplitude, mode-switching and triggering may also be predicted [5]. The fundamental basis of OSCILOS is similar to other thermoacoustic network modelling tools [7, 8], which have been validated and used extensively in a variety of problems.

## 2.2 Entropy wave advection model

OSCILOS accounts for one-dimensional entropy waves. These are assumed to be generated by the flame; they are negligible upstream of the flame and advect downstream of the flame. Although the entropy waves are assumed to be planar at their point of generation, 2-D/3-D effects can be partially accounted for using the Gaussian model described in Morgans et al. [4]. This incorporates entropy wave shear dispersion due to mean flow variations using the concept of an impulse response. A time-impulsive entropy fluctuation applied at the flame,  $\sigma_{\text{flame}}(t) = \delta(t)$ , assumed uniform over the combustor cross section, is transformed to a Gaussian-shaped “impulse response” at it advects downstream (again referring to strength averaged over a downstream plane), as shown in Fig. 2.

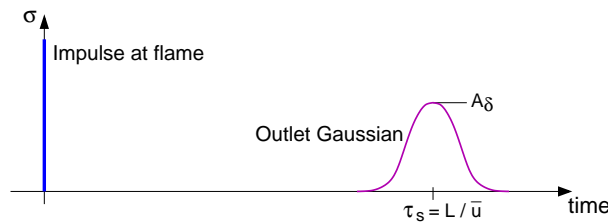


**Figure 2.** An entropy wave impulse applied at the flame gives rise approximately to a Gaussian-shaped entropy wave strength at combustor exit.

The entropy wave strength at the combustor exit, the location at which the choked acceleration boundary condition is applied, is then

$$(4) \quad \sigma_{\text{outlet}}(t) = A_\delta \exp(-\pi A_\delta^2 (t - \tau_s)^2) = \frac{1}{\sqrt{\pi} \Delta \tau_s} \exp\left(-\left(\frac{t - \tau_s}{\Delta \tau_s}\right)^2\right).$$

$A_\delta$  represents the maximum height of the Gaussian response, and  $\Delta\tau_s$  the dispersion time, such that  $\sigma_{\text{outlet}}(\tau_s + \Delta\tau_s) = A_\delta \exp(-1)$ . Note that dissipation is assumed negligible, so that the integral of the Gaussian is 1, the same as for the applied flame impulse.  $A_\delta$  and hence  $\Delta\tau_s$  can be deduced from the probability density function (PDF) of the residence time [3]. For a distance  $L$  along the combustor, the residence time is  $\tau_{\text{RES}}(r) = \frac{L}{u(r)}$ , where the velocity profile  $u(r)$  for a fully developed turbulent pipe flow is shown in Eq (5) and  $u_{\text{max}} = 1.2\bar{u}$ . The height of the PDF is then  $A_\delta$ , with  $\Delta\tau_s = 1/(\sqrt{\pi}A_\delta)$ .

$$(5) \quad u(r) = u_{\text{max}} - 2.5 \frac{u_{\text{max}}}{20} \ln\left(\frac{R}{R-r}\right)$$

### 3. Test Cases and Results

#### 3.1 The thermoacoustic modes of a model combustor

The effect of entropy noise on thermoacoustic modes has previously been considered using a rectangular pulse model for entropy wave advection [2], but with no systematic means of estimating the rectangular pulse height and spread. The present contribution is to implement the improved Gaussian entropy wave advection model described above [4], and to assess the effect of the shear dispersion associated with a real velocity profile.

We first consider a model combustor similar to Case 1 in Goh & Morgans [2]. The combustor geometry is shown in Figure 3, with the combustion and mean flow parameters summarised in Table 1. As in Case 1 of [2], choked upstream and downstream boundaries are applied, although the improved upstream choked boundary condition of [9] is used rather than the expression from [1]. The mean Mach number upstream of combustion is furthermore reduced to 0.08 to achieve a more realistic downstream Mach number. The flame model applied is an  $n - \tau$  model with first-order frequency fall-off; the gain  $n_f = 3$ ,  $\tau_f = 1\text{ms}$  and  $f_{\text{cutoff}} = 15.9\text{Hz}$ .

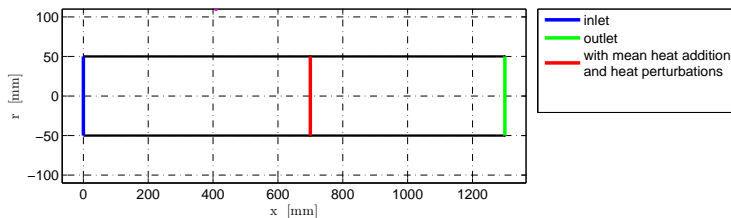


**Figure 3.** The model combustor geometry, including the location of the compact flame.

**Table 1.** Combustion (left) and mean flow (right) properties. The upstream (top row) flow parameters are set similar to Case 1 in [2]; the downstream (bottom row) values are calculated in OSCIOS.

Fuel	Equiv. ratio $\phi$ [-]	Comb. eff. $\eta$ [-]	$\bar{p}$ [Pa]	$\bar{T}$ [K]	$\bar{M}$ [-]	$c$ [m/s]	$\gamma$ [-]
Ethylene	0.7	0.855	$2 \times 10^5$	293	0.08	343	1.4
			$1.843 \times 10^5$	1785	0.208	847	1.4

For advective shear dispersion due to the mean turbulent velocity profile, the impulse response at combustor exit and corresponding flame-to-exit frequency response magnitude are shown in Figure 4. The corresponding dispersion time is  $\Delta\tau_s = 0.3818$  ms.

The variation of the thermoacoustic modes of the combustor with entropy wave advection model is shown in Fig. 5 and summarised in Table 2. It is clear that the entropy noise significantly affects the thermoacoustic modes, even when accounting for entropy wave shear dispersion due to the turbulent velocity profile.

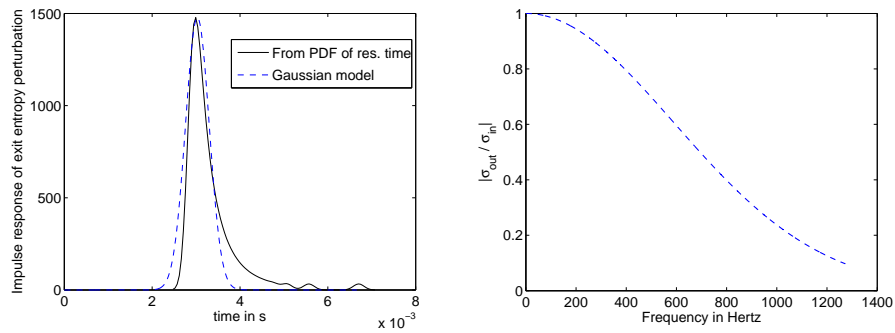


**Figure 4.** Left: The impulse response of entropy wave strength at combustor exit. Right: The flame-to-exit frequency response magnitude based on the Gaussian model.

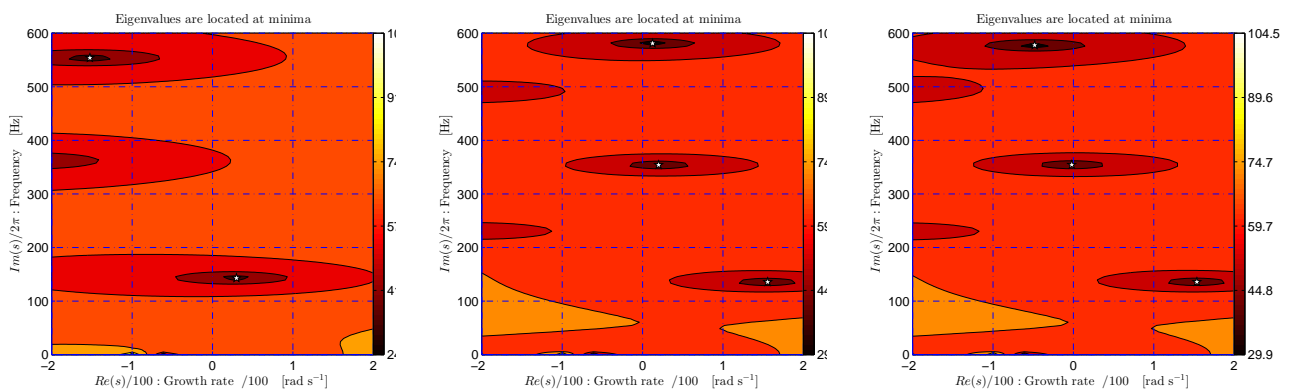


**Figure 5.** Thermoacoustic mode predictions. Left: no entropy noise. Middle: with entropy noise, assuming undispersed entropy waves. Right: with entropy noise, assuming entropy waves with advective shear dispersion.

**Table 2.** The main thermoacoustic modes of the model combustor

Entropy waves?	Frequency [Hz]	Growth rate [rad/s]
No	143.9	31.2
	552.6	-141.7
Yes - uniform advection	136.0	154.9
	354.1	25.1
	580.2	12.3
Yes - turbulent shear dispersion	136.3	152.9
	354.5	3.6
	576.6	-47.3

It has previously been suggested that shear dispersion will have greater effect for long combustors, meaning that the effect of entropy noise on thermoacoustic modes can be neglected for long combustor geometries. Indeed, the shear dispersion and hence rate of frequency fall off (see Figure 4 right) will increase with combustor length - the fall off depends on reduced frequency,  $f_{red} = fL/U$ . However, the modal frequencies of long combustors are correspondingly reduced – for longitudinal modes they decrease as  $f_{mode} \propto 1/L$ . The thermoacoustic modes of long combustors therefore may not be significantly less affected by entropy noise, and this will form the basis of the second investigation.

### 3.2 The thermoacoustic modes of industrial gas turbine combustor test cases

We now perform a study on a set of test cases representative of cannular industrial gas turbine combustors. The length downstream of combustion,  $L$ , is varied substantially, from  $L = 0.4\text{m}$  to  $L = 1.2\text{m}$ , a representative range for industrial combustors. A fully developed turbulent pipe flow profile is used to deduce the advective shear dispersion for each combustor length. The combustor geometry for the shortest of the lengths is shown in Figure 6. The combustion and mean flow parameters are summarised in Table 3; note that  $c_p$  and hence  $\gamma$  both vary with temperature [6].

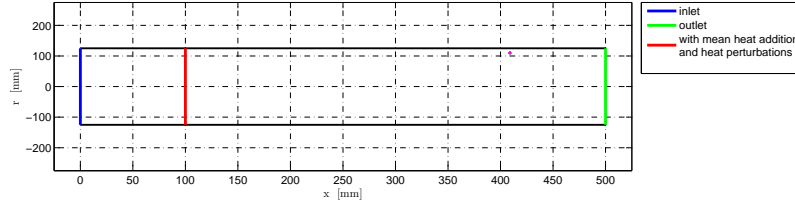


**Figure 6.** Left: The geometry (for  $L = 0.4\text{m}$ ) of the industrial representative combustor.

**Table 3.** Combustion (left) and mean flow (right) parameters. The upstream (top row) mean flow parameters are prescribed, the downstream (bottom row) are calculated within OSCILOS.

Fuel	Equiv. ratio $\phi$ [-]	Comb. eff. $\eta$ [-]	$\bar{p}$ [Pa]	$\bar{T}$ [K]	$\bar{M}$ [-]
Methane	0.7	0.8	$15 \times 10^5$	500	0.08
			$14.66 \times 10^5$	1722.1	0.157

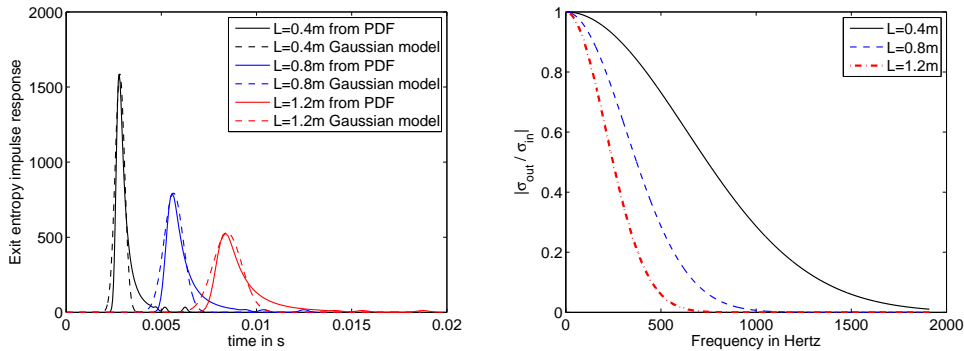


**Figure 7.** Left: The impulse response of entropy wave strength at combustor exit. Right: The flame-inlet frequency response magnitude based on the Gaussian model.

Closed upstream and choked downstream acoustic boundary conditions are applied. An  $n - \tau$  flame model with first-order frequency fall-off is used; a gain  $n_f = 1$  is used for all combustor lengths, but the time delay,  $\tau_f$ , and cut-off frequency,  $f_{\text{cutoff}}$ , depend on the combustor length, such that  $\tau_f = [3, 3, 1]$  ms and  $f_{\text{cutoff}} = [300, 230, 230]$  Hz for  $L = [0.4, 0.8, 1.2]$  m. The entropy wave strength impulse responses at exit and corresponding frequency responses are shown in Figure 7. The dispersion times are  $\Delta\tau_s = [0.356, 0.712, 1.068]$  ms for  $L = [0.4, 0.8, 1.2]$  m.

The thermoacoustic modes for all three combustor lengths are compared in Figure 8. When entropy noise is neglected, all of the thermoacoustic modes are stable, with the dominant mode frequency reducing with combustor length, as expected. Accounting for entropy noise in the presence of advective shear dispersion results in mode destabilisation for all three lengths. The changes in the dominant mode are summarised in Table 4 below.

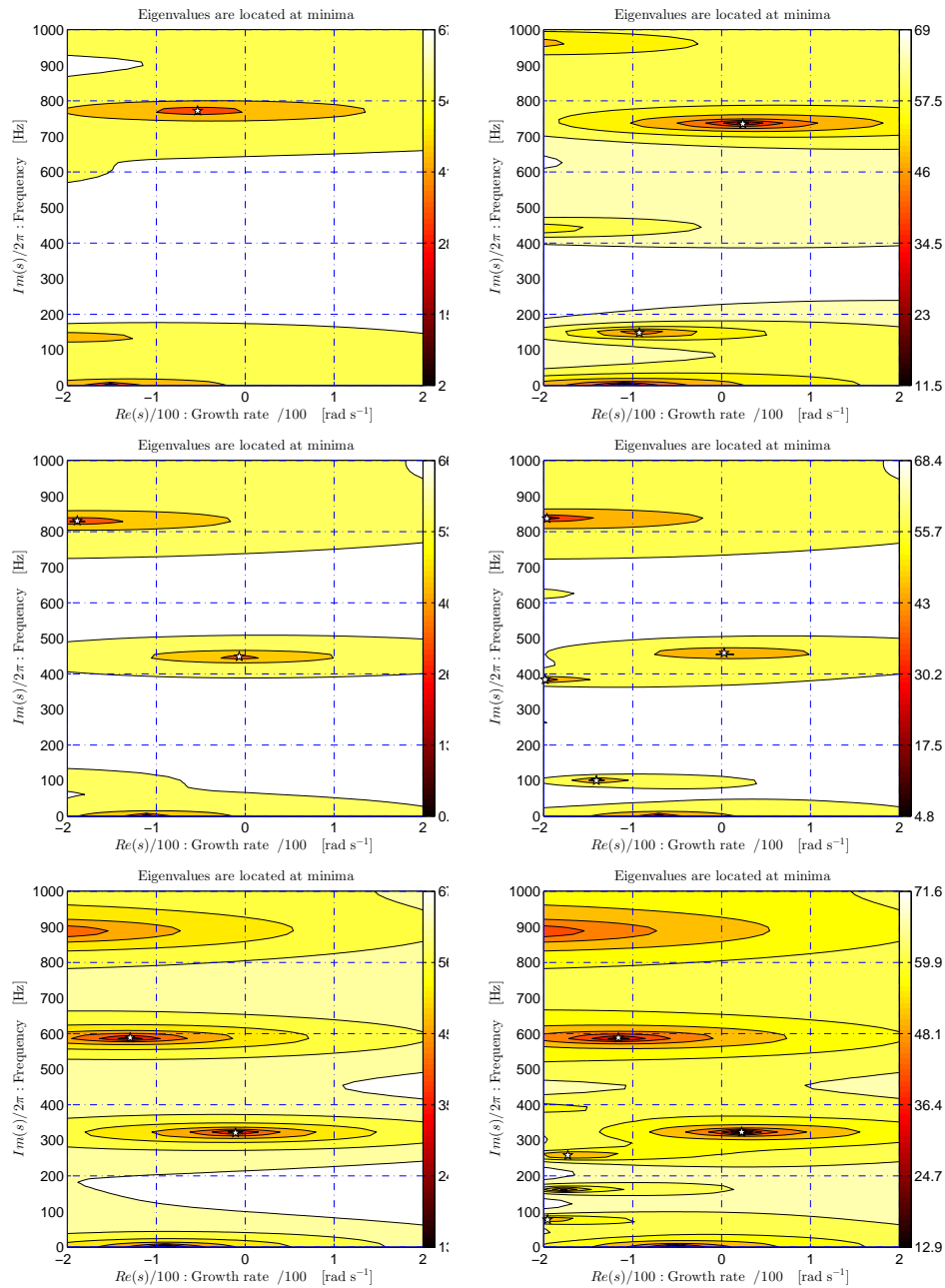


**Figure 8.** Thermoacoustic mode predictions. Top:  $L = 0.4$  m. Middle:  $L = 0.8$  m. Bottom:  $L = 1.2$  m. Left plots: entropy noise neglected. Right plots: entropy noise accounting for, with advective shear dispersion of entropy waves.

**Table 4.** The main thermoacoustic mode of the industrial combustor test cases

Case	Frequency [Hz]	Growth rate [rad/s]
$L = 0.4\text{m}$ , no entropy noise	771.8	-53.5
$L = 0.4\text{m}$ , with entropy noise	735.4	+23.9
$L = 0.8\text{m}$ , no entropy noise	448.6	-6.7
$L = 0.8\text{m}$ , with entropy noise	458.9	+2.9
$L = 1.2\text{m}$ , no entropy noise	320.1	-10.9
$L = 1.2\text{m}$ , with entropy noise	323.1	+22.6

## 4. Conclusions

For a typical gas turbine combustor exhibiting downstream flow acceleration, there are two sources of noise arising from unsteady combustion. The first and better understood source is the noise generated by the flame itself. The second source arises when the temperature fluctuations generated by the flame, also known as “entropy waves”, advect downstream and are accelerated. The noise generated by the acceleration of these entropy waves depends crucially on the advection process between the flame, where the entropy waves are generated, and the combustor exit, where they are accelerated. The present work has investigated the extent to which the reflected component of “entropy noise” affects the thermoacoustic modes of typical combustor, in the context of recent improvements in advection models.

An improved model for the entropy wave advection process, based on a fully developed turbulent velocity profile, was incorporated into a low order network modelling tool for predicting the thermoacoustic modes of a combustor. A range of test combustor geometries and flow conditions were investigated, some of which were intended to be representative of industrial combustors. The findings suggested that for all representative combustor lengths, entropy wave shear dispersion due to advection is sufficiently weak that thermoacoustic modes may be strongly affected by entropy noise. The work has considered only fully developed turbulent velocity profiles; it would be interesting to consider typical mean flow profiles for real combustors, exhibiting more complex hydrodynamic flow features.

The authors would like to acknowledge the financial support of the ERC Starting Grant ACOULO-MODE (2013-18).

## REFERENCES

1. Marble F. E. and Candel S. M. Acoustic Disturbance from Gas Non-Uniformities Convected Through a Nozzle, *J. of Sound and Vib.*, **55**, 225–243, (1977)
2. Goh C. S. and Morgans A. S. The influence of entropy waves on the thermoacoustic stability of a model combustor, *Combustion Science and Technology*, **185**, 249–268, (2013)
3. Sattelmayer T. Influence of the combustor aerodynamics on combustion instabilities from equivalence ratio fluctuations, *ASME J. Eng. Gas Turbines Power*, **125**, 11–19, (2003)
4. Morgans A. S., Goh C. S. and Dahan J. A. The dissipation and shear dispersion of entropy waves in combustor thermoacoustics, *J. of Fluid Mechanics*, **733**, (2013)
5. Li J. and Morgans A. S. Time domain simulations of nonlinear thermoacoustic behaviour in a simple combustor using a wave-based approach, *J. of Sound and Vib.*, doi:10.1016/j.jsv.2015.01.032 (2015)
6. Li J., Yang D., Luzzato C. M. A. and Morgans A. S. *Tech Report: OSCILOS: the open source combustion instability low order simulator*, <http://www.oscilos.com>, (2014)
7. Stow S. R. and Dowling A. P. A time-domain network model for nonlinear thermoacoustic oscillations, *ASME J. Eng. Gas Turbines Power*, **131**, (2009)
8. Schuermans B., Bellucci V. and Paschereit C. O. Thermoacoustic modelling and control of multi burner combustion systems, *Proc. of ASME Turbo Expo*, GT2003-38688 (2003)
9. Stow S. R., Dowling A. P. and Hynes T. P. Reflection of circumferential modes in a choked nozzle, *J. of Fluid Mechanics*, **467**, 215–239, (2002)